applied sciences

IMPACT FACTOR 1.689

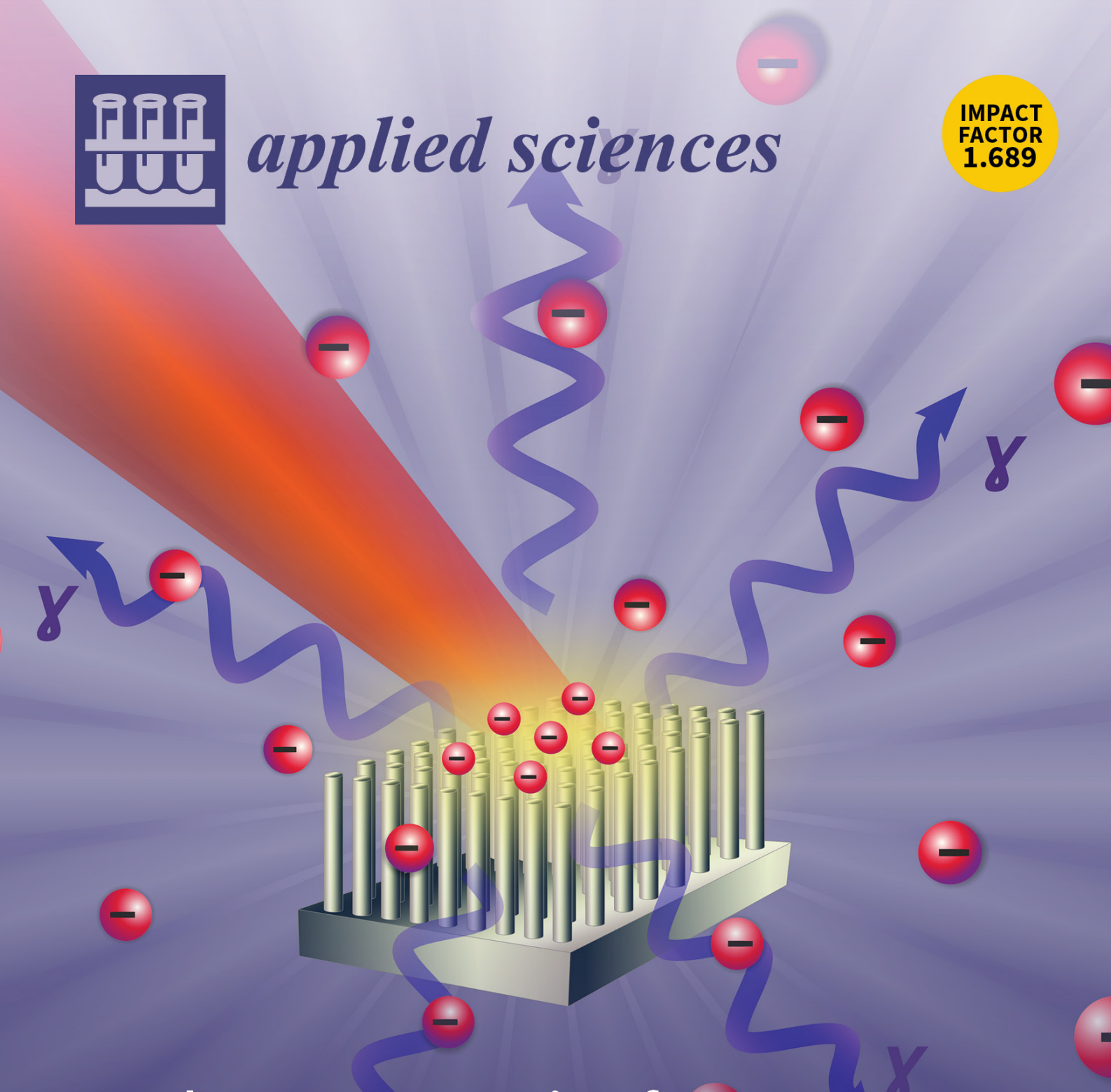

Hard X-ray Generation from ZnO Nanowire Targets in a Non-Relativistic Regime of Laser-Solid Interactions

Volume 8 · Issue 10 | October 2018

MDPI

mdpi.com/journal/applsci
ISSN 2076-3417

applied sciences

MDPI

Article

New Generation of Electrochemical Sensors Based on Multi-Walled Carbon Nanotubes

Thiago M. B. F. Oliveira [1] and Simone Morais [2,*]

[1] Centro de Ciência e Tecnologia, Universidade Federal do Cariri, Av. Tenente Raimundo Rocha, Cidade Universitária, Juazeiro do Norte 63048-080, CE, Brazil; thiago.mielle@ufca.edu.br

[2] REQUIMTE–LAQV, Instituto Superior de Engenharia do Porto, Instituto Politécnico do Porto, Rua Dr. Bernardino de Almeida 431, 4249-015 Porto, Portugal

* Correspondence: sbm@isep.ipp.pt; Tel.: +351-22-8340500; Fax: +351-22-8321159

Received: 13 August 2018; Accepted: 12 October 2018; Published: 15 October 2018

Abstract: Multi-walled carbon nanotubes (MWCNT) have provided unprecedented advances in the design of electrochemical sensors. They are composed by sp^2 carbon units oriented as multiple concentric tubes of rolled-up graphene, and present remarkable active surface area, chemical inertness, high strength, and low charge-transfer resistance in both aqueous and non-aqueous solutions. MWCNT are very versatile and have been boosting the development of a new generation of electrochemical sensors with application in medicine, pharmacology, food industry, forensic chemistry, and environmental fields. This work highlights the most important synthesis methods and relevant electrochemical properties of MWCNT for the construction of electrochemical sensors, and the numerous configurations and successful applications of these devices. Thousands of studies have been attesting to the exceptional electroanalytical performance of these devices, but there are still questions in MWCNT electrochemistry that deserve more investigation, aiming to provide new outlooks and advances in this field. Additionally, MWCNT-based sensors should be further explored for real industrial applications including for on-line quality control.

Keywords: nanomaterials; multi-walled carbon nanotubes; synthesis methods; electrochemical properties; electrochemical sensors; electroanalysis; sensing applications

1. Introduction

Several nanomaterials have been exploited for different purposes, but carbon nanotubes (CNT) and their composites emerged as the most exciting and versatile [1–5]. CNT are carbon allotropes with intermediate properties between graphite and fullerenes [6]. They are composed by sp^2 carbon units oriented as one (single-walled; SWCNT) or multiple concentric tubes (multi-walled; MWCNT) of rolled-up graphene, separated by ≈0.35 nm [4,6–8]. Both nanostructures had positive impacts for the applied sciences, but the latter has gained more attention due to the higher yield and lower production cost per unit, thermochemical stability, and ability to maintain or improve its electrical properties when submitted to different functionalization processes [9]. A general MWCNT representation and the possible π- and σ-covalent bonds established along the nanostructure are displayed in Figure 1. MWCNT also present remarkable active surface area, chemical inertness, high strength, and low charge-transfer resistance in both aqueous and non-aqueous solutions, making them suitable for numerous applications as nano-sized metallic and/or semiconducting components in transistors [10], energy storage [11], hybrid conductors [12], supercapacitors [13], thin-film coatings [2,5,6], field emitters [14], (bio)fuel cells [1–3,7], photovoltaic devices [1,3], electromagnetic shields [1,7], and electrochemical probes [1,2,5–7].

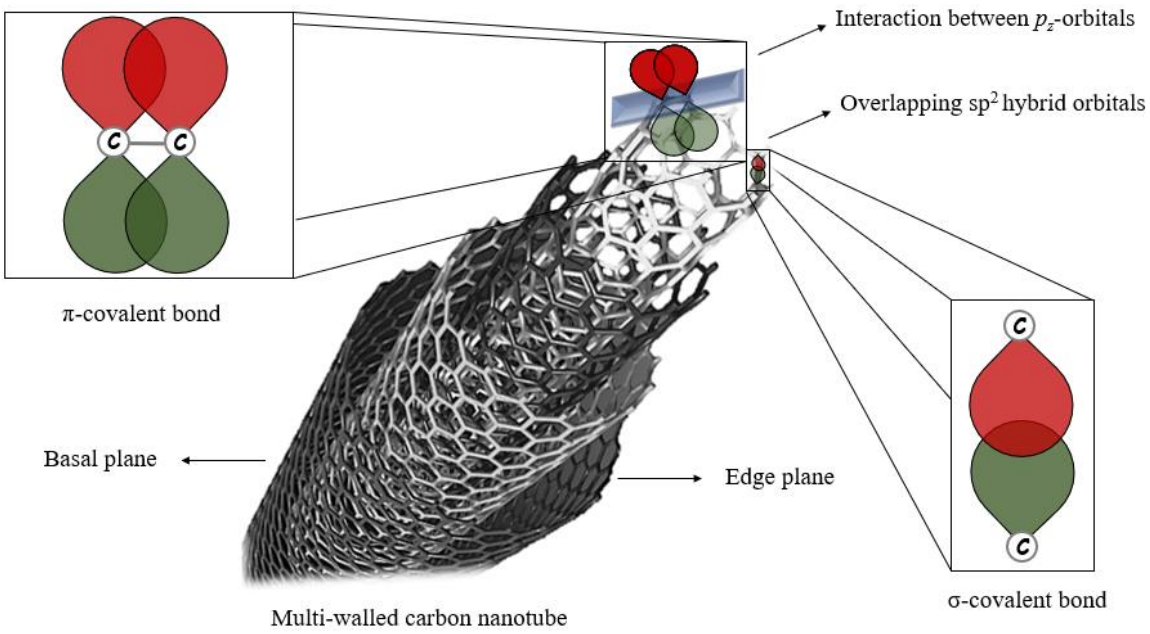

Figure 1. Representative structure of non-continuous multi-walled carbon nanotubes, emphasizing the different types of orbital interactions, as well as σ- and π-covalent bonds established along the 1D carbon networks.

MWCNT provide a series of functionalities to the electrochemical sensors, making them fantastic devices for analytical purposes. Electrochemical sensors are by definition, according the International Union of Pure and Applied Chemistry, "electrochemical devices that transform the effect of the electrochemical interaction analyte-electrode into a useful analytical signal" [15]; these effects may be promoted electrically or may be caused by a spontaneous interaction at the zero-current condition [15]. Thus, electrochemical sensors may be organized in four main subgroups: voltammetric, potentiometric, potentiometric solid electrolyte gas sensors, and chemically sensitized field effect transistor [15]. MWCNT associate high surface area (about 1600 m^2 g^{-1}) and exceptional electrical conductivity (current densities as high as 10^9 A cm^{-2}), which suit them to the miniaturization and portability of the systems [14].

Nowadays, electrochemical MWCNT-based sensors have demonstrated remarkable applications in medicine, clinical diagnostics, pharmacology, food industry, sanitary surveillance, occupational safety, forensic chemistry, and environmental analysis [1–3,6–9,15–18]. Other promising innovations can also be found in review papers that have been published over the last decade [6–9,15–20]. The assays are performed by various electrochemical techniques (voltammetry, amperometry, potentiometry, impedance spectroscopy, and their associations), which are selected according to the nature of the target-redox process [2,6,7,15–20]. MWCNT bring together high electronic conductivity, large specific surface area, chemical stability, biocompatibility, and ease of modification, improving the intensity and resolution at which the electroanalytical signals are observed on the working platforms [15–18]. However, the successful application requires a refined control of the sensor architecture and physicochemical properties, as well as the functionalization and/or surface modification of the carbon nanotubes [4,6–9]. Thus, in this study, these critical variables will be highlighted and discussed, addressing exciting issues from the MWCNT synthesis to their application in electrochemical biosensors design. With this goal in mind, the available literature concerning this subject in Thomson Reuters, *Web of Science* was reviewed from 2013 to March 2018.

2. MWCNT Synthesis Methods

Regarding synthesis methods, there are different paths that can be followed, such as electrical arch-discharge (EAD), laser ablation (LA), and numerous types of chemical vapor deposition (CVD), so that MWCNT conductor character varies according to the diameter and degree of helicity [4,7,21]. An overall layout of each system and its associated processes are shown in Figure 2. The yield rate of all aforementioned methods is more than 75% under appropriate operating conditions [22], but some questions about the structural quality, diameter uniformity, chirality, practicality, number of unitary operations, and production cost continue to divide opinions about the best strategy [4,21–24]. Researchers are continually trying to explore each possibility to optimize or innovate them for several new applications.

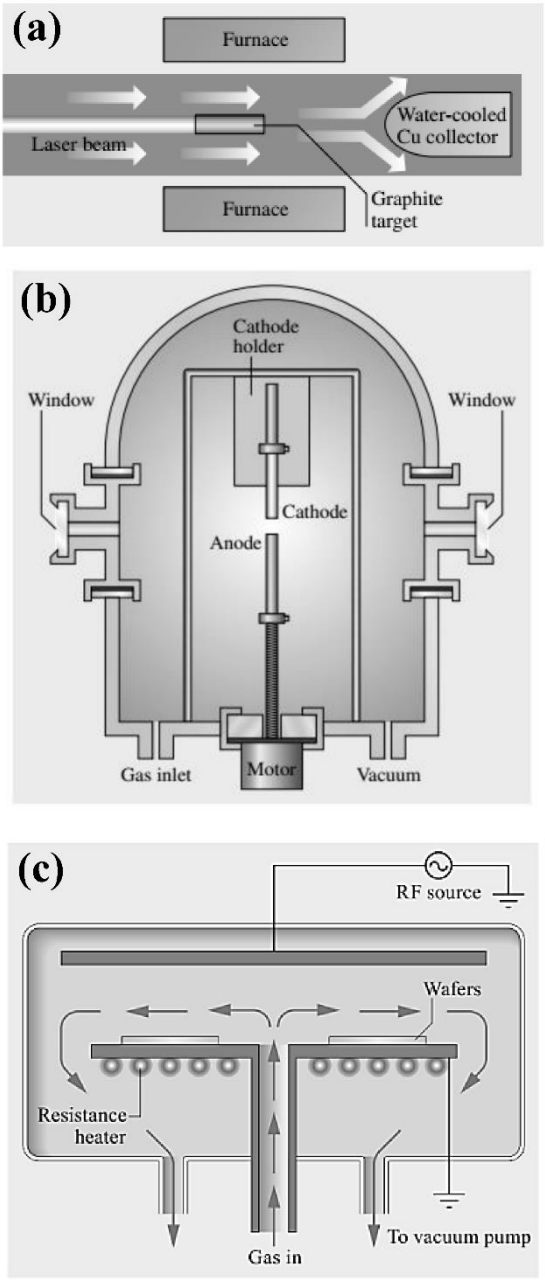

Figure 2. General layout of an (**a**) electrical arch-discharge (adapted by permission from Reference [23]), (**b**) laser ablation (adapted by permission from Reference [23]) and (**c**) chemical vapor deposition apparatus (adapted by permission from Reference [25]) used to synthesize multi-walled carbon nanotubes.

EAD is relatively less expensive, offers better yield quality, but involves high temperature for synthesis [21–23]. Triggering an electrical arc-discharge between two electrodes, a plasma composed by carbon and metallic catalysts vapor (iron, nickel, cobalt, yttrium, boron, cerium, among others) is formed under a rare gas atmosphere (helium or argon) [21–23]. The vapor content is a consequence of the energy transferred to the catalysts-doped anode, causing its erosion, while MWCNT are formed as a hard and consistent deposit on the cathode [23]. The LA method also represents a promising alternative to synthesize high-quality carbon nanotubes at room temperature, although it demands high instrumental and operational costs [21–23]. In this technique, a pulsed or continuous laser beam is focused on catalyst-based graphite pellet, which is placed at the center of a quartz tube filled with an inert gas and kept at 1200 °C. The radiant energy is enough to sublimate the carbon substrate, and this vapor is swept by the gas flow towards the conical water-cooled copper collector. MWCNT deposits are formed in the majority on the same collector, but appreciable amounts are also found on the quartz tube walls and graphite pellet backside. Both EAD and LA also produce in parallel other carbon phases and all products contain metallic impurities from the catalysts [23]. The small fractions of remaining metals do not compromise the performance of the electrochemical devices, and there are several purification processes proposed in the literature and by some commercial companies to remove undesirable phases [22–24]. Nevertheless, these procedures are based on oxidation under strong acidic conditions, which may significantly affect the integrity of the nanostructures.

The synthesis performed by CVD overcomes the aforementioned difficulties, guarantees large-scale production and, for these reasons, it has become more widely used to obtain MWCNT [22–25]. This technique involves either a heterogeneous (if a solid substrate is used) or a homogeneous process (supposing that reactions takes place in the gas phase) [23,25]. The main synthetic route explores the catalytic decomposition of a carbon-containing source on substrates containing transition metals and their composites (Au, Ag, Cu, Cr, Co, Fe, Mn, Mo, Ni, Pt, Pd, SiO_2, SiC, and ceramics), which enables the growth of aligned and dense arrays of nanotubes [23,24]. Alternative energy sources such as plasma and optical excitation can also be employed, giving the possibility to synthesize MWCNT at low-temperatures (450–1000 °C) compared to EAD and LA [23–25]. The CVD method also allows greater control of selectivity/type, homogeneity and size of the nanotubes (a few tens to hundreds of micrometers) in comparison to the others, although these characteristics are strongly dependent on the nature and structure of the catalysts, and the operational conditions of the synthesis. All these aspects affect the density and speed of electron transfer through the nanostructures that, in turn, directly impact the performance of the electrochemical sensors.

3. MWCNT Electrochemical Properties

MWCNT-based electrochemical sensors have remarkable advantages for analytical applications, such as enhanced detection sensitivity, low charge-transfer resistance (R_{tc}), electrocatalytic effect, and reduced fouling. It is also speculated that traces of metallic catalysts can add remarkable electroanalytical characteristics (positive synergistic effect) to the nanotubes, playing a supporting role for the development of the devices [6,7,15–26]. There are still controversies about the electron transfer mechanism along the structural network: Some researchers believe that the sidewalls of the CNT are inert (i.e., the edge–plane-graphite-like open ends and defect sites control the phenomenon) [26–28], but some studies conducted with two-dimensional SWCNT have shown evidence of charge-transfer on the basal-plane [7,23,25]. Although the uncertainties about the fundamental contributions of MWCNT in electrochemical sensors, the number of MWCNT successful applications in highly complex systems does not stop growing [2,9,17,26].

Understanding the size-dependent features is an indispensable requirement to explore the fascinating properties of nanotubes in analytical tools and to move the electroanalytical researches forward. In this sense, it must be assumed that the electronic band structure of CNT as a hexagonal lattice, where each carbon atom is covalently bonded to three others via sp^2 molecular orbitals (the fourth valence electron in a p_z-orbital hybridizes with all others to form a delocalized π-band) [27].

Like this, an even number of electrons are contained in the basic nanotube structure, whose conduction character will depend on its behavior as metal or semiconductor. This property can be assessed through the tight-binding electronic structure calculations, considering the translational vector (C_h) that connects two equivalent crystallographic sites (unitary vectors a_1 and a_2) and its coefficients (n_1 and n_2), according to the following Equation (1):

$$C_h = n_1 a_1 + n_2 a_2 \tag{1}$$

so that a metallic behavior is observed when the result is an integer multiple of three, while a non-metallic/semiconductor profile is observed for other cases; a direct consequence of the different conduction band gaps [6]. The electron-transfer along the MWCNT are also influenced by the tube diameter (d_t), chiral angle (θ), and basic translation vector (T), as shown in Figure 3. Thus, the manner in which a graphene sheet is rolled determines the main electronic properties of the resulting nanotube [6,15,23,27].

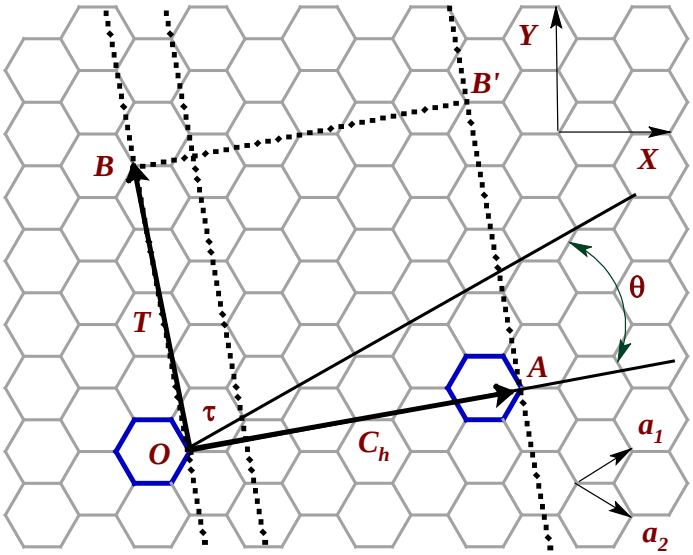

Figure 3. Honeycomb lattice structure of graphene and the main parameters that control the chirality and electronic properties of the resultant nanotube (adapted by permission from References [8,23]).

Observing the referred parameters on the tubulene lattice, d_t values can be determined by Equations (2) and (3), which relate this variable with the circumferential length of the nanotube (L) and a hexagonal network constant (a):

$$d_t = \frac{L}{\pi} = \frac{C_h}{\pi} = \frac{a\left(n_1^2 + n_1 n_2 + n_2^2\right)^{\frac{1}{2}}}{\pi} \tag{2}$$

considering $a_\circ = 1.42$ Å for carbon nanotubes [6]:

$$a = \sqrt{3} a_\circ = 2.49 \text{ Å} \tag{3}$$

Regarding the θ, the expression that describes its magnitude can be written as follows:

$$\cos\theta = \frac{2n_1 + n_2}{2\sqrt{n_1^2 + n_1 n_2 + n_2^2}} \tag{4}$$

The vector T is used to specify the orthogonal orientation to the C_h axis of the nanotube, and its value can be calculated by:

$$T = \frac{(2n_2 + n_1)a_1 - (2n_1 + n_2)a_2}{d_k} \quad (5)$$

where d_k ranging from d (when $n_1 - n_2$ and d_k is not a multiple of $3d$) to $3d$ (when $n_1 = n_2$ and d_k is a multiple of $3d$) for chiral tubulenes, considering d the greatest common divisor for the coefficients n_1 and n_2 [6,15,23,27].

In addition, a translation vector (τ) is also necessary to delimit the unitary cell of the nanotube. It can be represented by Equations (6)–(8),

$$\tau = t_1 a_1 + t_2 a_2 \quad (6)$$

$$t_1 = \frac{(2n_2 + n_1)}{d_r} \quad (7)$$

$$t_2 = \frac{-(2n_1 + n_2)}{d_r} \quad (8)$$

knowing that d_r (d–$3d$) is the greatest common divisor of the respective coefficients. In summary, the limits of the 1D nanotube unit cell (plane segment *OAB'BO*) are demarcated by the vectors C_h and T, whereas a_1 and a_2 define the area of the 2D graphene unit cell [6,27]. This sequence of equations is very important for the development of electrochemical sensors because it allows to determine the number of electric and phononic bands in the carbon nanostructures, i.e., the magnitude of the electrical conduction through the nanomaterial.

The influence of the band structure on the nanotube conduction bands is defined in the context of the Fermi velocity (υ_F).

$$\upsilon_F = \frac{\hbar k_F}{m} \quad (9)$$

where $\hbar$ is the reduced Planck constant, k_F is the Fermi wavevector, and m represents the mass of the nanostructure under study. These values are not well-defined in cases where the Fermi surface is non-spherical, but it is estimated to be $\upsilon_F \sim 10^6$ ms^{-1} for semiconductors or even higher for conductors [27]. This prevision corroborates the observation recorder in the density of states diagram for SWCNT with different chirality, since at the Fermi energy level (E_F) there is a finite electronic transition for metallic structures (first van Hove optical transition), but a zero-band gap for semiconductors (second van Hove optical transition). A general description of the band structures and density of states for metallic and semiconductor nanotube is presented in Figure 4. Thus, if we imagine that MWCNT are composed by several coaxial SWCNT, it might be expected that they are not strictly a 1D-type conductor [7,27]. Likewise, when the nanotubes have different chirality, the band structure undergoes alterations, and the resultant coupling between the electronic states at the E_F and phonon modes may cause superconductivity [4,7,27]. Despite the similarity with metallic materials, the carrier density in carbon nanotubes (1D quantum wires) is much lower and novel physical electron-electron phenomena (such as spin-charge separation and suppression of the electron tunneling density of states) should be considered to justify the possible discrepancies, as predicted by Luttinger liquid theory [23,26–28].

Some electrochemical studies showed a lower R_{tc} for MWCNT containing structural defects and/or traces of metallic impurities (catalyst nanoparticles), so that the current flow occurs mainly through the outer most nanotube cylinder [26–28]. Only one of the concentric tubes needs to exhibit this behavior for the overall electronic properties to be essentially metallic-low quantum capacitance values [7,27]. It is believed that if d_t is smaller than the elastic mean free path, the one-dimensional ballistic transport predominates, but the opposite characterizes a two-dimensional diffusive current flow [7,26–28]. In addition, nanotubes with larger d_t have a greater density of structural defects, besides facilitating their modification and functionalization, which are interesting requirements for the development of electroanalytical devices [2,6–9]. The mean length of the nanotubes also has a significant effect on the electron-transfer rate; they are inversely proportional

properties [22,24,27]. Vertically aligned structures also exhibit superior performance compared to those randomly immobilized [2,16,25–28].

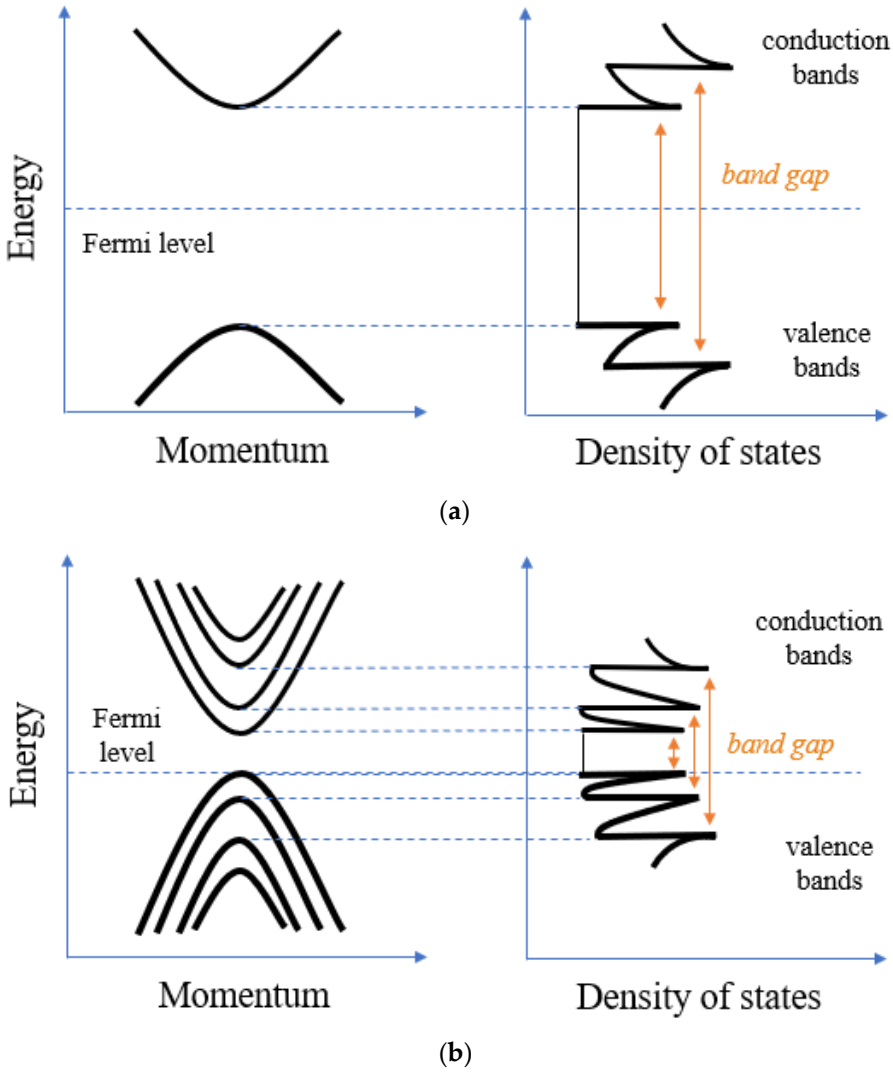

Figure 4. Idealized models of band structures and density of states for (**a**) metallic and (**b**) semiconducting nanotubes.

Therefore, MWCNT provide special characteristics in electrochemical sensors both in aqueous and non-aqueous electrolytes (electrocatalytic properties, high and fast electron-transfer, signal amplification and stability, among other particularities observed in different prototypes) when compared with the conventional carbonaceous electrodes (such as glassy carbon, highly-oriented pyrolytic graphite, carbon microfiber, and boron-doped diamond) [26–28]. However, the true reasons and fundamental electrochemical properties responsible for the reported performances (both when nanotubes are used alone or in (nano)composites) are still not fully elucidated and demand further research [2,4,6,9,17].

4. Overview of MWCNT Applications in Electrochemical Sensors

Different and exciting properties are obtained with macro-, micro-, and nano-structured carbon derivatives [4,17], but the implementation of the latter in the configuration of electrochemical sensors brought new opportunities to detect trace concentrations (μmol L^{-1} to pmol L^{-1}) of numerous analytes (active principle and metabolites of drugs, personal care products, flame retardants, gases, surfactants,

industrial additives, polycyclic aromatic hydrocarbons (PAHs), polychlorinated biphenyls (PCBs), hormones, pesticides, among others) in complex matrices (natural waters, soils, foodstuffs, biological fluids, fuels, wastes, and even in living organisms) [1–17]. This trend led to the development of the newest category of electroanalytical devices (third generation/way), i.e., nanotools for nanoscale analysis [2,16]. The basic mechanism for the operation of these tools is based on the conversion of redox processes, registered at the sensor/electrolyte interface, onto quantitative or semi-quantitative information. MWCNT had an important role to reach such advances, and this fact can be easily attested by the exceptional growth of scientific reports in this field [2–6,8,16,17]. MWCNT's large active surface area, facile electron-transfer with a variety of molecules, and their use in nano-composites (mixed with conductive polymers, nanoparticles and active biomolecules), as well as their high potential for device miniaturization, have been enhancing the sensitivity of current methodologies and providing new sensing opportunities [2,17,19–22]. The multichannel electron ballistic transport and the presence of holes/defects along the structures, especially when functionalized with carboxyl groups and their derivatives, further enhance the previously mentioned properties [2,4–9]. When converting a graphene sheet to a nanotube, one electron of the carbon atoms remains in *p*-orbitals, organized between valence (π) and conduction (π^*) bands with very low bandgap (a partial σ–π hybridization), which favors a fast electron transfer. The density of states in MWCNT structure depends on diameter (≈2–100 nm), chirality/configuration (concentric, herringbone, and bamboo) and nature (semiconductor, conductor, and superconductor) [1,7,15]. In addition, the strength of C−C bonds is among the most robust and, when they are organized in the nanotube form, these interactions also provide flexibility and resistance to rupture, increasing the versatility and number of possible applications of these nanomaterials [4,7,16].

Electrochemical sensing of a wide variety of chemically, biologically, and environmentally important analytes was investigated on MWCNT (chemical purity ≥95%)—based solid electrodes, as shown in Table 1. Numerous traditional and modern pharmaceuticals, for instance, are electroactive on these sensors and relevant contributions have been reported, either in stationary or in flow-through systems. Mao et al. [29] fabricated an electrochemical sensor for metronidazole (antibacterial and anti-inflammatory compound employed for the treatment of protozoal diseases) based on MWCNT and chitosan (CTS)-nickel complex modified glassy carbon electrode (GCE) by the self-assembly technique. The polymer matrix facilitates the immobilization of the nanocomposite on the electrode support, while the association between nickel and carbon nanomaterials increases the current intensity of the electroanalytical signal. Using differential pulse voltammetry (DPV), Ni-CTS/MWCNT/GCE also showed electrocatalytic effect toward metronidazole reduction, making the method highly selective to its analysis in pharmaceutical and biological samples, with a low detection limit (LOD; 0.025 μmol L^{-1}) and suitable reproducibility and stability. Holanda et al. [30] reported a simple methodology to quantify acetaminophen (a compound with analgesic and antipyretic action) in commercial formulations, using a GCE modified with gold nanoparticles (Au-NP), functionalized MWCNT (*f*-MWCNT) and cobalt phthalocyanine (Co-Pht) as working sensor. Using *f*-MWCNT, a lower system capacitance and better stability of the sensor was observed. The quantification of acetaminophen on Co-Pht/*f*-MWCNT/Au-NP/GCE was carried out by square-wave voltammetry (SWV) that, in turn, showed a sensitivity (LOD = 0.135 μmol L^{-1}) and reproducibility similar to the standard ultraviolet-visible spectrophotometric procedure (at the wavelength of 257 nm). Montes et al. [31] studied the superior electrochemical activity of MWCNTs with shorter dimensions (diameter × length: 100–170 nm × 5–9 μm and 6–9 nm × 5 μm) towards the oxidation of propionic acid derivatives, which are drugs with analgesic, antipyretic, and anti-inflammatory properties. Electrochemical impedance spectroscopy (EIS) and cyclic voltammetric (CV) data showed better electrocatalysis effect, R_{tc} and signal amplification for the sensor constructed with the shorter diameter nanostructures due to the increased defect density revealed by Raman spectroscopic measurements. The developed sensor (MWCNT (diameter × length: 6–9 nm × 5 μm)/GCE) was adapted to a flow-injection analysis system (FIA) and provided a sensitivity and accuracy to determine ibuprofen (LOD = 1.9 μmol L^{-1})

by amperometry comparable to that obtained by capillary electrophoresis. Pavinatto et al. [32] used a fluorine doped tin oxide (FTO) electrode, coated with nanostructured layer-by-layer films of CTS@MWCNT (Figure 5), as a sensor for 17-α-ethinylestradiol, that is a synthetic estrogen widely used as an oral contraceptive. The electron-transfer on the sensor reduced dramatically in the presence of the nanotubes, improving its electroanalytical performance and enabling assays at very low concentrations. Using the irreversible and adsorption-controlled oxidation process of the estrogen onto the three-bilayer CTS@MWCNT/FTO, it was possible to determine it by SWV (LOD = 0.09 μmol L^{-1}) without significant effect of the most common interfering compounds present in human urine (urea, uric, and ascorbic acids, glucose, NaCl, KCl, and NH_4Cl). Chen et al. [33] used a nanocomposite based on MWCNT and 1-octyl-3-methyl-imidazolium hexa-fluorophosphate ionic liquid (IL) to modify a GCE, to develop a chiral electrochemical sensor for the enantiomeric recognition of propranolol, using the linear sweep voltammetry (LSV) technique. The authors did not present a LOD but declared the success of the proposed method to evaluate the enantiomeric purity of reagents and wastewater treatment efficiency. Other promising MWCNT-based electrochemical devices were also reported to successfully analyze hydrochlorothiazide and triamterene [34], mangiferin and icariin [35], natamycin [36], omeprazole [37], gentamicin [38], and many other drugs [2,6,9,17–20], attesting their electroanalytical performance and effectiveness.

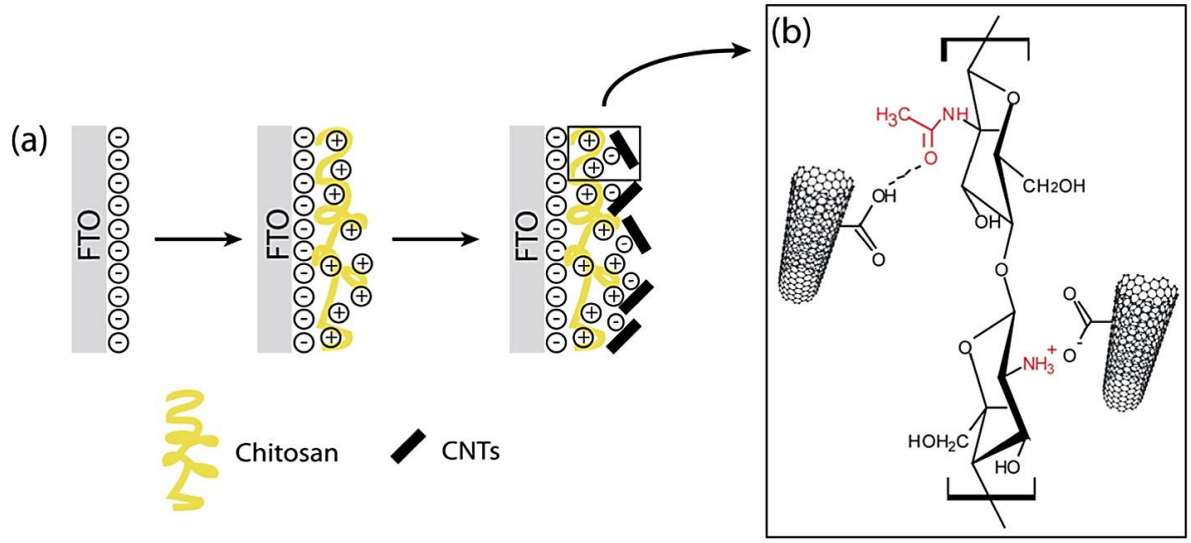

Figure 5. (**a**) Schematic representation of the layer-by-layer and (**b**) supramolecular interaction between chitosan and multi-walled carbon nanotubes (MWCNT) for 1-bilayer film (adapted by permission from Reference [32]).

The growing trend of using miniaturized systems for the electroanalysis of bioactive molecules in living organisms through less invasive tests has positive repercussion and wide acceptance [2,17]. From this perspective, glucose sensors have been receiving special attention, since these analytic tools can be used as an effective way to diagnose diabetes, hypoglycemia, and other metabolic diseases in real time, using human blood and other secreted fluids as study matrix. Başkaya et al. [39] fabricated a non-enzymatic glucose sensor using a hybrid film (composed by *f*-MWCNT and highly monodisperse nickel nanoparticles) immobilized on GCE, which was able to determine this target in human blood serum samples by amperometry, with sensitivity (LOD = 0.021 μmol L^{-1}) and stability similar to one of commercial enzymatic biosensors. The results also support the positive synergistic effects that are observed when different nanomaterials are associated into the same matrix, enhancing the capacity and versatility of the electrochemical sensors. Purine bases are also crucial biomolecules to the immune function and abnormal changes causes serious disorders, such as cancer, epilepsy, lupus erythematous, renal calculi, and cardiovascular alterations. Wang et al. [40] prepared a nanocomposite by mixing

MWCNT and copper-nickel hybrid nanoparticles (Cu@Ni-NP), which was deposited onto a GCE surface, with the goal of monitoring adenine and guanine in ds-DNA from mice brain tissues. Using DPV under the optimized conditions, the Cu@Ni-NP/MWCNT/GCE sensor achieved a LOD of 0.17 μmol L^{-1} and 0.33 μmol L^{-1} for guanine and adenine, respectively, attesting to its potential to quantify purine bases in complex samples. Likewise, sensors for point-of-care detection of DNA damage in medical diagnostics are also on the rise. Li and Lee [41] investigated the performance of *f*-MWCNT (functionalization with oxygen-containing groups to improve the immobilization and stability of the bioelement) as an additive in electrochemical DNA sequence differentiation ability. The electroanalytical signal achieved by DPV was highly selective and modulated between the probe (5′-GTG TTG TCT CCT AGG TTG GCT CTG-3′; 24-base fraction of the p53 gene, used as a marker for breast cancer) and its complementary sequence (5′-CAG AGC CAA CCT AGG AGA CAA CAC-3′). The detection capacity (LOD = 141.2 pmol L^{-1}) was more than two orders better than the previously reported for graphene functionalized (*f*-Grf) based sensors, even in the presence of single (5′-CAG AGC CAA CCT CGG AGA CAA CAC-3′) and all-base mismatched pairs (5′-ATA TCG ACC TTG GCC GAG ACG GTG-3′). Great effort has also been directed towards the development of electrochemical devices capable of early detection of immune deficiency diseases, such as acquired immune deficiency syndrome (AIDS) caused by the HIV-retrovirus. Ma et al. [42] proposed a device composed by a GCE modified with MWCNT and molecularly imprinted polymers (MIPs) based on CTS for the determination of HIV-p24 protein in real human serum samples (Figure 6). Using DPV and the developed sensor (HIV-p24/CTS/MWCNT/GCE), a low limit of detection (0.083 pg cm^{-3}), good selectivity, repeatability, reproducibility, stability, and accuracy were reached for the proposed electroanalysis; validation was performed by comparative studies with enzyme-linked immunosorbent assay (ELISA). The outstanding ability of MWCNT-based electrochemical sensors to simulate redox reactions that occur in vivo has also been demonstrated with the electroanalysis of hemoglobin [43], amino acids [44], cholesterol [45], bilirubin [46], neurotransmitters, and related compounds [47–49], and even microorganisms [50], in mammalian fluid samples, achieving great results and contributing to the early diagnosis and treatment of several related diseases.

The occurrence of pesticides in foodstuffs, natural water, soils, among other matrices of environmental relevance, constitute a worldwide concern. Sipa et al. [51] associated square-wave adsorptive stripping voltammetry (SWAdSV) and a modified sensor (β-cyclodextrins/MWCNT/GCE) to determine trace concentrations of the pesticide dichlorophen. The excellent electroanalytical performance of the system, mainly in the presence of nanotubes (LOD = 4.4 × 10^{-8} mol L^{-1}), allowed to monitor this vermicide in river water (Pilica River, in Poland) with good selectivity and absence of natural and anthropogenic interfering compounds. Özcan and Gürbüz [52] developed a simple and sensitive sensor for the voltammetric determination of the herbicide clopyralid in urine, river water, sugar beet, wheat, and herbicide formulations (Phaeton® and Lontrel™). This novel sensor was built by modification of a GCE with a nanocomposite containing acid-activated MWCNT (oxygen-functionalized nanostructures with very low R_{tc}) and fumed silica, which, when associated with DPV, attained a LOD of 0.8 nmol L^{-1}, confirming the sensitivity of the proposed method. Ghodsi and Rafati [53] reported a strategy to develop a voltammetric sensor for diazinon (an organophosphate insecticide) based on TiO_2 nanoparticles (TiO_2-NP) and MWCNT nanocomposite assembled onto a GCE. Under optimum conditions, TiO_2-NP@MWCNT/GCE reached a LOD of 3.0 nmol L^{-1}, using both CV and SWV, and this performance was explored for the electroanalysis of the pesticide in well and tap water. Other mentioned advantages were the fast response time, good repeatability, stability, besides the fast and inexpensive electrode modification. Sensitive electrochemical sensors that associate the unique properties of MWCNT and metallic nanoparticles were also proposed by Wei et al. [54] and Ertan et al. [55], aiming to electroanalysize trichlorfon insecticide (LOD = 4.0 × 10^{-7} mol L^{-1}, using Nafion®/TiO_2-NP@MWCNT@carboxymethyl chitosan/GCE) and simazine herbicide (LOD = 2.0 × 10^{-11} mol L^{-1}, using MIP/platinum nanoparticles@polyoxometalate@*f*-MWCNT/GCE), respectively, reinforcing the positive synergistic effect between these nanostructures for the improvement of the electroanalytical methodologies.

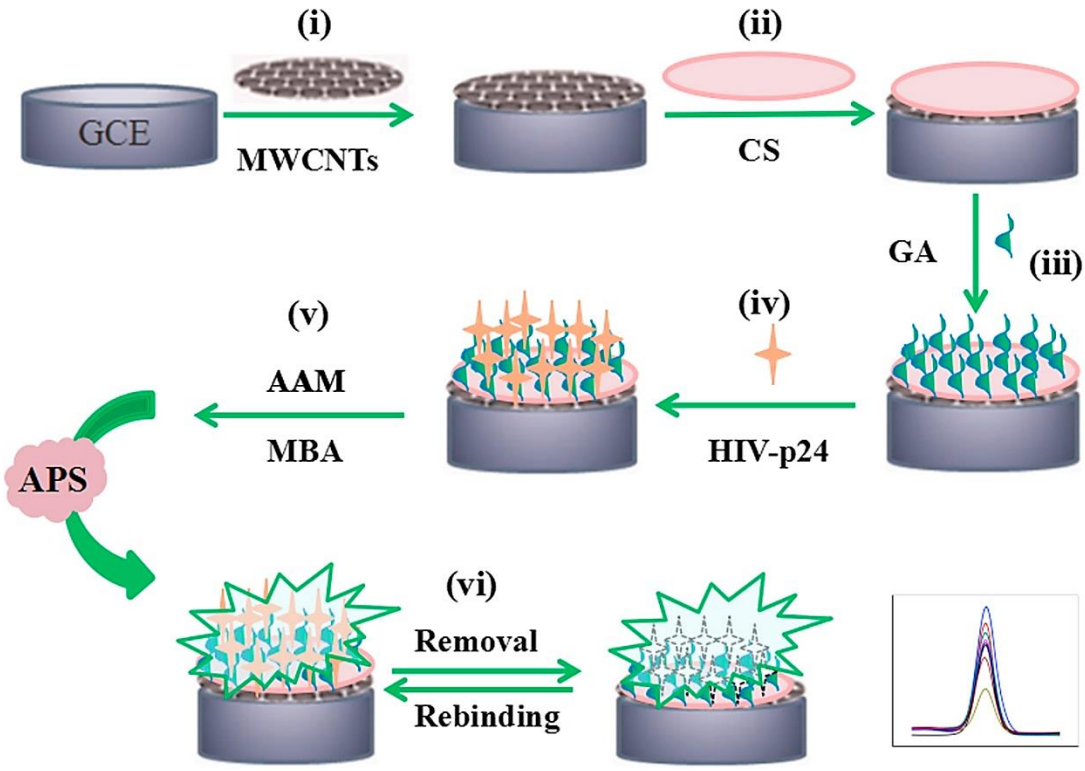

Figure 6. Detailed procedure diagram for fabrication of the HIV-p24/CTS/MWCNT/GCE sensor (adapted by permission from Reference [42]).

The wide active area and low R_{tc} observed for MWCNT, and related (nano)composites, have been providing important advances on the single and simultaneous electroanalytical quantification of metallic cations (Cd^{2+} [56], Pb^{2+} [56], Mn^{2+} [57], and Na^{+} [58]) and anions (SO_3^{2-} [59], NO_2^{-} [60], and BrO_3^{-} [60]) in varied and complex matrices (wastewater [57], drinking water [56], and groundwater [58,59]). Trace concentrations of persistent organic pollutants (sunset yellow [61], tartrazine [62], and luteolin [62] dyes), as far as gases (chlorine [63], carbon dioxide [64], and methanol vapor [65]) and industrial by-products (glycerol [66], bisphenol A [67], hydrazine [68], and hydrogen peroxide [69]) are now being monitored with MWCNT-based sensors in a quick, reproducible, reliable, and cost-effective way when compared to the traditional analytical protocols, including those based on electrochemical devices from previous generations.

Table 1. Configuration, analytical performance and application of electrochemical sensors based on multi-walled carbon nanotubes.

Sensor	Modification Procedure	Analyte(s)	Technique(s)/Detection Limit	Application	Stability	Reference
		Pharmaceuticals				
Ni-CTS/MWCNT/GCE	GCE modified with MWCNT and Ni-CTS complex through drop coating and self-assembly, respectively	metronidazole	DPV/0.025 μmol L^{-1}	tablet and biological samples	81% after one month	[29]
Co-Pht@*f*-MWCNT/Au-NP/GCE	suspension of Co-Pht and *f*-MWCNT immobilized on Au-NP modified GCE by drop coating	acetaminophen	SWV/0.135 μmol L^{-1}	commercial formulations	n.r.	[30]
MWCNT(shorter diameter)/GCE	MWCNT (diameter × length: 6–9 nm × 5 μm) dropped on GCE	ibuprofen	CV/1.90 μmol L^{-1}	tablet and liquid commercial formulations	n.r.	[31]
Three bilayer MWCNT@CTS/FTO	FTO coated with nanostructured Layer-by-Layer films of MWCNT@CTS	17-α-ethinylestradiol	SWV/0.09 μmol L^{-1}	synthetic urine samples	n.r.	[32]
MWCNT@IL/GCE	immobilization of MWCNT and IL (1-octyl-3-methyl-imidazolium hexa-fluorophosphate) nanocomposite on GCE	propranolol	LSV/n.r.	commercial reagent and wastewater	n.r.	[33]
MWCNT/GCE	suspension of MWCNT dropped on GCE	hydrochlorothiazide and triamterene	ASV/2.8 × 10^{-8} and 2.9 × 10^{-8} mol L^{-1} for hydrochlorothiazide and triamterene, respectively	hemodialysis samples	n.r.	[34]
Au@Ag-NP/MWCNT-SGSs/GCE	layer-by-layer assembly of Au@Ag-NP and MWCNT-SGSs on GCE	mangiferin and icariin	DPV/0.017 μmol L^{-1} for both compounds	*Rhizoma anemarrhenae*, *Artemisia capillaris Herba* and *Epimedium macranthum* samples	≤95.1% after one month	[35]
3D-Grf@MWCNT/GCE	electrodeposition of 3D-Grf@MWCNT suspension on GCE	natamycin	LSV/1.0 × 10^{-8} mol L^{-1}	red wine and beverage samples	94.6% after two weeks	[36]
Fe_3O_4-NP@MWCNT/PDDA/GCE	casting of PDDA modified GCE with Fe_3O_4-NP@MWCNT hybrid film	omeprazole	LSV/15 nmol L^{-1}	tablet, capsules, wastewater, serum, and urine	92.1% after three weeks	[37]
Calixarene/MWCNT/SPE	dip coating of graphite-based SPE in composite matrix of calixarene and MWCNT	gentamicin sulphate	potentiometry/7.5 × 10^{-8} mol L^{-1}	dosage forms and spiked surface water samples	n.r.	[38]
		Biologically active molecules				
Ni-NP@*f*-MWCNTs/GCE	drop coating of hybrid film (Ni-NP and *f*-MWCNT) on GCE	glucose	CV and amperometry/0.021 μmol L^{-1}	human blood serum samples	practically constant signal after 1000th cycle	[39]
Cu@Ni-NP/MWCNT/GCE	immobilization of hybrid film of Cu@Ni-NP and MWCNT on GCE	guanine and adenine	DPV/0.17 μmol L^{-1} and 0.33 μmol L^{-1} for guanine and adenine, respectively	ds-DNA from mice brain tissues	96.7% for 30 days	[40]
Gold electrode	measurements with unmodified gold electrode, keeping *f*-MWCNT additive and DNA sequence in electrolyte solution	breast cancer marker (5′-GTG TTG TCT CCT AGG TTG GCT CTG-3′; 24-base fraction of the p53 gene)	DPV/141.2 pmol L^{-1}	solution containing the complementary sequence (5′-CAG AGC CAA CCT AGG AGA CAA CAC-3′)	n.r.	[41]

Table 1. *Cont.*

Sensor	Modification Procedure	Analyte(s)	Technique(s)/Detection Limit	Application	Stability	Reference
HIV-p24/MIP /MWCNT/GCE	HIV-p24 crosslinking MIP (acrylamide functional monomer, *N*,*N*′-methylenebisacrylamide as crosslinking agent and ammonium persulphate as initiator) immobilized on MWCNT/GCE	HIV-p24 protein	DPV/0.083 pg cm^{-3}	real human serum samples	98.6% after 10 days	[42]
MIP/MWCNT/Cu	MIP (itaconic acid monomer, ethylene glycol dimethacrylate cross-linker and α,α′-azobisisobutyronitrile as initiator) on MWCNT modified Cu electrode	hemoglobin	potentiometry/1.0 μg mL^{-1}	human bile juice and urine samples	6 months without significant change in the electrode performance	[43]
Cu-MP@polyethylenimine /MWCNT/GCE	Cu-MP dispersed in polyethylenimine and dropped on MWCNT/GCE	amino acids, albumin and glucose	SWV and amperometry/0.10–0.37 μmol L^{-1} for the amino acids (L-cystine, L-histidine and L-serine); 1.2 mg mL^{-1} for albumin; and 182 nmol L^{-1} for glucose	pharmaceutical products and beverages	7.7% RSD after 10 successive calibration plots using the same surface	[44]
MIP/Au-NP/MWCNT/GCE	Au-NP electrodeposited on MWCNT/GCE, and assembled with MIP (tetrabutylammonium perchlorate)	cholesterol	DPV/3.3 × 10^{-14} mol L^{-1}	n.r.	91.7% after one month	[45]
MWCNT/SPE	MWCNT films casted onto SPE	bilirubin	CV/9.4 μmol L^{-1}	n.r.	n.r.	[46]
Grf-Ox@MWCNT/GCE	drop coating of Grf-Ox@MWCNT suspension on GCE	catechol and dopamine	CV/n.r.	n.r.	n.r.	[47]
Phenazine methosulfate/3-aminophenylboronic acid/*f*-MWCNT/GCE	drop coating of phenazine methosulfate and 3-aminophenyl boronic acid on *f*-MWCNT/GCE	NADH	amperometry/0.16 μmol L^{-1}	human serum	96.7% after five consecutive measurements	[48]
HPU/β-CD/MWCNT@Nafion®/GCE	layer-by-layer of HPU, β-CD and composite film (MWCNT@Nafion®) on GCE	uric acid	amperometry/n.r.	n.r.	n.r.	[49]
		Microorganisms				
MWCNT@Nafion®/GCE	dip coating of composite suspension (MWCNT@Nafion®) on GCE	Enterotoxigenic *Escherichia coli* F4 (K88)	SWV/6 × 10^{4} CFU mL^{-1}	swine stool samples	n.r.	[50]
		Pesticides				
β-CD/MWCNT/GCE	β-CD and MWCNT composite suspension dropped on GCE	dichlorophen	SWAdSV/ 4.4 × 10^{-8} mol L^{-1}	river water	93.9% after one week	[51]
Fumed silica/acid-activated MWCNT/GCE	drop coating of a nanocomposite suspension (Fumed silica and acid-activated MWCNT) on GCE	clopyralid	DPV/0.8 nmol L^{-1}	urine, river water, sugar beet, wheat, and herbicide formulations (*Phaeton* and *Lontrel*)	91% after three weeks	[52]
TiO_2-NP@MWCNT/GCE	TiO_2-NP@MWCNT nanocomposite dropped on GCE	diazinon	CV an SWV/3.0 nmol L^{-1}	well and tap water	89% after 28 days	[53]
Nafion®/TiO_2-NP@MWCNT @carboxymethyl chitosan/GCE	Nafion® assembled on composite film (TiO_2-NP@MWCNT @carboxymethyl chitosan) previously immobilized on GCE	trichlorfon	DPV/4.0 × 10^{-7} mol L^{-1}	apple, mushroom, and cucumber	98% after one week	[54]
MIP/Pt-NP@polyoxometalate@*f*-MWCNT/GCE	MIP (pyrrole in the presence of the analyte) assembled on hybrid film (Pt-NP@polyoxometalate@*f*-MWCNT) immobilized on GCE	simazine	DPV/2.0 × 10^{-11} mol L^{-1}	wastewater samples	96.9% after 45 days	[55]

Table 1. *Cont.*

Sensor	Modification Procedure	Analyte(s)	Technique(s)/Detection Limit	Application	Stability	Reference
		Metallic cations				
BiF/Grf-Red/MWCNT/SPE	layer-by-layer of BiF, Grf-Red and MWCNT on SPE (gold support)	Cd^{2+} and Pb^{2+}	SWV/0.6 ppb for Cd and 0.2 ppb for Pb	drinking water	n.r.	[56]
Mn^{2+}-imprinted polymer /IL@CTS@MWCNT/GCE	thermal immobilization of Mn^{2+}-imprinted polymer on composite layer (IL@CTS@MWCNT) dropped on GCE	Mn^{2+}	SWAdSV/0.15 μmol L^{-1}	wastewater	94.8% after two weeks	[57]
β-NiO_x/MWCNT-modified CPE	electrodeposition of hybrid film of β-NiO_x on MWCNT-modified CPE	Na^+	SWV/9.86 × 10^{-8} mol L^{-1}	groundwater	practically constant signal for more than five hundred consecutive cycles	[58]
		Anions				
f-MWCNT/GCE	drop coating of *f*-MWCNT (COOH-functionalized structures) as suspension on GCE	SO_3^{2-} and NO_2^-	DPV/215 nmol L^{-1} for SO_3^{2-} and 565 nmol L^{-1} for NO_2^-	groundwater	≥96.4% after one week	[59]
Ag-NP@MWCNT/GCE	drop coating of nanocomposite (Ag-NP@MWCNT) on GCE	BrO_3^-	amperometry/n.r.	n.r.	n.r.	[60]
		Dyes				
Grf-Ox@MWCNT/GCE	suspension of Grf-Ox@MWCNT immobilized on GCE by drop coating	sunset yellow and tartrazine	LSV/0.025 μmol L^{-1} for sunset yellow and 0.010 μmol L^{-1} for tartrazine	orange juice	89–93% after one month	[61]
Poly(crystal violet)/MWCNT/GCE	electropolymerization of crystal violet on MWCNT/GCE	luteolin	DPV/5.0 × 10^{-9} mol L^{-1}	Chrysanthemum samples	93% after one month	[62]
		Gas/Vapor				
Hexa-decafluorinated zinc phthalocyanine @*f*-MWCNT/SPE (gold support)	drop coating of the composite (Hexa-decafluorinated zinc phthalocyanine@*f*-MWCNT) on SPE	Cl_2	resistance/0.06 ppb	n.r.	n.r.	[63]
SbSI@CNTs/Au-microelectrode	ultrasonic bonding of SbSI@CNTs composite on Au-microelectrode	CO_2	amperometry/n.r.	n.r.	n.r.	[64]
MWCNT@polyaniline/FTO	drop coating of MWCNT@polyaniline nanocomposite on FTO	methanol vapor	resistance/≈50 ppm	n.r.	the signal remained almost constant for up to 20 days	[65]
		Industrial by-products				
CuO-NP/MWCNT/GCE	electrodeposition of CuO-NP on MWCNT/GCE	glycerol	amperometry/5.8 × 10^{-6} g dm^{-3}	biodiesel samples	n.r.	[66]
Au-NP/Grf-Red@MWCNT/GCE	electrodeposition of Au-NP on Grf-Red@MWCNT/GCE	bisphenol A	DPV/1.0 × 10^{-9} mol L^{-1}	river water and shopping receipt samples	98% after 30 days	[67]
Pd-NP/Grf-Red@MWCNT/GCE	electrodeposition of Pd-NP on Grf-Red@MWCNT/GCE	hydrazine	amperometry/0.15 μmol L^{-1}	tap water spiked with hydrazine	n.r.	[68]
Prussian blue/CTS@MWCNT /GCE	electrodeposition of Prussian blue complex on GCE Modified with CTS@MWCNT nanocomposite	hydrogen peroxide	amperometry/0.10 μmol L^{-1}	routine analysis in pure electrolyte	90.5–92.6% after two weeks	[69]

Au-NP: gold nanoparticles; Ag-NP: silver nanoparticles; Cu-MP: copper microparticles; CuO-NP: copper oxide nanoparticles; Pd-NP: palladium nanoparticles; CTS: chitosan; Co-Pht: cobalt phthalocyanine; IL: ionic liquid; HPU: hydrothane polyurethane; β-CD: β-cyclodextrin; BiF: bismuth film; MIP: molecular imprinted polymer; MWCNT: multi-walled carbon nanotubes; *f*-MWCNT: functionalized multi-walled carbon nanotubes; 3D-Grf: three-dimensional graphene; Grf-Ox: graphene oxide; Grf-Red: reduced graphene; HIV-p24: retrovirus of the AIDS; GCE: glassy carbon electrode; SPE: screen-printed electrode; CPE: carbon paste electrode; FTO: fluorine doped thin oxide electrode; LSV: linear sweep voltammetry; CV: cyclic voltammetry; DPV: differential pulse voltammetry; SWV: square-wave voltammetry; ASV: adsorptive stripping voltammetry; SWAdSV: square-wave adsorptive stripping voltammetry; n.r.: no reported.

5. Final Remarks

MWCNT and their (nano)composites have been the origin for exciting and versatile sensing platforms due to their inherent advantages, namely large active surface area, electrocatalytic properties, high and fast electron-transfer, signal enlargement, reduction of the overpotential, chemical inertness, among others. Their incorporation into electrochemical sensors has been improving the electroanalytical performance of these devices and simultaneously widening their scope and range of applications. However, some limitations related to the high cost of production of high purity MWCNT have been restricting their large-scale and industrial utilization. Thus, improvements on the current synthetic routes and purification methods or/and development of novel low cost and effective techniques are clearly needed. In addition, comprehensive characterization of the toxicity of MWCNT is another requirement to expand their application to in vivo assays. These achievements will contribute to the construction of reliable and reproducible MWCNT-based electrochemical sensors enlarging sensors exploitation in real in vivo monitoring and in on-line manufacturing applications.

Author Contributions: Conceptualization, T.M.B.F.O. and S.M.; Data curation, T.M.B.F.O.; Supervision, Simone Morais; Writing—original draft, T.M.B.F.O.; Writing—review and editing, S.M.

Funding: Simone Morais is grateful for financial support from the European Union (FEDER funds through COMPETE) and National Funds (Fundação para a Ciência e Tecnologia-FCT) through projects UID/QUI/50006/2013 and AAC No. 02/SAICT/2017—project No. 029547 "CECs(Bio)Sensing—(Bio)sensors for assessment of contaminants of emerging concern in fishery commodities", by FCT/MEC with national funds and co-funded by FEDER. She also thanks financial support by Norte Portugal Regional Operational Programme (NORTE 2020), under the PORTUGAL 2020 Partnership Agreement, through the European Regional Development Fund (ERDF): projects Norte-01-0145-FEDER-000011 and Norte-01-0145-FEDER-000024.

Acknowledgments: T.M.B.F. Oliveira thanks the Brazilian agencies CNPq, CAPES and FUNCAP for all scientific support to his projects with nanostructured materials.

Conflicts of Interest: The authors declare no conflict of interest.

References

1. Sudha, P.N.; Sangeetha, K.; Vijayalakshmi, K.; Barhoum, A. Nanomaterials history, classification, unique properties, production and market. In *Emerging Applications of Nanoparticles and Architecture Nanostructures—Current Prospects and Future Trends*; A Volume in Micro and Nano Technologies; Makhlouf, A.S.H., Barhoum, A., Eds.; Elsevier: Cambridge, MA, USA, 2018; pp. 341–384, ISBN 978-0-323-51254-1.
2. Soriano, M.S.; Zougagh, M.; Valcárcel, M.; Ríos, Á. Analytical Nanoscience and Nanotechnology: Where we are and where we are heading. *Talanta* **2018**, *177*, 104–121. [CrossRef] [PubMed]
3. Adams, F.C.; Barbante, C. Nanoscience, nanotechnology and spectrometry. *Spectrochim. Acta Part B* **2013**, *86*, 3–13. [CrossRef]
4. Liu, J.; Liu, L.; Lu, J.; Zhu, H. The formation mechanism of chiral carbon nanotubes. *Physica B* **2018**, *530*, 277–282. [CrossRef]
5. Kurkowska, M.; Awietjan, S.; Kozera, R.; Jezierska, E.; Boczkowska, A. Application of electroless deposition for surface modification of the multiwall carbon nanotubes. *Chem. Phys. Lett.* **2018**, *702*, 38–43. [CrossRef]
6. Zaporotskova, I.V.; Boroznina, N.P.; Parkhomenko, Y.N.; Kozhitov, L.V. Carbon nanotubes: Sensor properties. A review. *Mod. Electron. Mater.* **2016**, *2*, 95–105. [CrossRef]
7. Dumitrescu, I.; Unwin, P.R.; Macpherson, J.V. Electrochemistry at carbon nanotubes: Perspective and issues. *Chem. Commun.* **2009**, 6886–6901. [CrossRef] [PubMed]
8. Hamada, N.; Sawada, S.-I.; Oshiyama, A. New one-dimensional conductors: Graphitic microtubules. *Phys. Rev. Lett.* **1992**, *68*, 1579–1581. [CrossRef] [PubMed]
9. Mao, J.; Wang, Y.; Zhu, J.; Yu, J.; Hu, Z. Thiol functionalized carbon nanotubes: Synthesis by sulfur chemistry and their multi-purpose applications. *Appl. Surf. Sci.* **2018**, *447*, 235–243. [CrossRef]
10. Xiao, Z.; Elike, J.; Reynolds, A.; Moten, R.; Zhao, X. The fabrication of carbon nanotube electronic circuits with dielectrophoresis. *Microelectron. Eng.* **2016**, *164*, 123–127. [CrossRef]
11. Su, L.; Wang, X.; Wang, Y.; Zhang, Q. Roles of carbon nanotubes in novel energy storage devices. *Carbon* **2017**, *122*, 462–474. [CrossRef]

12. Guo, Y.; Shen, G.; Sun, X.; Wang, X. Electrochemical aptasensor based on multiwalled carbon nanotubes and graphene for tetracycline detection. *IEES Sens. J.* **2015**, *15*, 1951–1958. [CrossRef]
13. Liu, L.; Niu, Z.; Chen, J. Flexible supercapacitors based on carbon nanotubes. *Chin. Chem. Lett.* **2018**, *29*, 571–581. [CrossRef]
14. Parveen, S.; Kumar, A.; Husain, S.; Husain, M. Fowler Nordheim theory of carbon nanotube based field emitters. *Phys. B Condens. Matter.* **2017**, *505*, 1–8. [CrossRef]
15. Hulanicki, A.; Glab, S.; Ingman, F. Chemical sensors: Definitions and classification. *Pure Appl. Chem.* **1991**, *63*, 1247–1250. [CrossRef]
16. Kim, S.N.; Rusling, J.F.; Papadimitrakopoulos, F. Carbon nanotubes for electronic and electrochemical detection of biomolecules. *Adv. Mater.* **2007**, *19*, 3214–3228. [CrossRef] [PubMed]
17. López-Lorente, Á.; Valcárcel, M. The third way in analytical nanoscience and nanotechnology: Involvement of nanotools and nanoanalytes in the same analytical process. *Trends Analyt. Chem.* **2016**, *75*, 1–9. [CrossRef]
18. Harris, P.J. Engineering carbon materials with electricity. *Carbon* **2017**, *122*, 504–513. [CrossRef]
19. Abdalla, S.; Al-Marzouki, F.; Al-Ghamdi, A.A.; Abdel-Daiem, A. Different technical applications of carbon nanotubes. *Nanoscale Res. Lett.* **2015**, *10*, 1–10. [CrossRef] [PubMed]
20. Park, S.; Vosguerichian, M.; Zhenan Bao, Z. A review of fabrication and applications of carbon nanotube film-based flexible electronics. *Nanoscale* **2013**, *5*, 1727–1752. [CrossRef] [PubMed]
21. Rezaee, S.; Ghaderi, A.; Boochani, A.; Solaymani, S. Synthesis of multiwalled carbon nanotubes on Cu-Fe nano-catalyst substrate. *Res. Phys.* **2017**, *7*, 3640–3644. [CrossRef]
22. Dhore, V.G.; Rathod, W.S.; Patil, K.N. Synthesis and characterization of high yield multiwalled carbon nanotubes by ternary catalyst. *Mater. Today Proc.* **2018**, *5*, 3432–3437. [CrossRef]
23. Monthioux, M.; Serp, P.; Flahaut, E.; Razafinimanana, M.; Laurent, C.; Peigney, A.; Bacsa, W.; Broto, J.-M. Introduction to carbon nanotubes. In *Springer Handbook of Nanotechnology*, 2nd ed.; Bhushan, B., Ed.; Springer: Berlin, Germany, 2007; pp. 47–118, ISBN 3-540-29855-X.
24. Araga, R.; Sharma, C.S. One step direct synthesis of multiwalled carbon nanotubes from coconut shell derived charcoal. *Mater. Lett.* **2017**, *188*, 205–207. [CrossRef]
25. Rius, G.; Baldi, A.; Ziaie, B.; Atashbar, M.Z. Introduction to micro-/nanofabrication. In *Springer Handbook of Nanotechnology*, 4th ed.; Bhushan, B., Ed.; Springer: Berlin, Germany, 2017; pp. 51–86, ISBN 978-3-662-54355-9.
26. Yáñez-Sedeño, P.; Pingarrón, J.M.; Riu, J.; Rius, F.X. Electrochemical sensing based on carbon nanotubes. *Trends Anal. Chem.* **2010**, *29*, 939–953. [CrossRef]
27. Bandaru, P.R. Electrical properties and applications of carbon nanotube structures. *J. Nanosci. Nanotechnol.* **2007**, *7*, 1–29. [CrossRef]
28. Ahammad, A.J.S.; Lee, J.-J.; Rahman, M.A. Electrochemical sensors based on carbon nanotubes. *Sensors* **2009**, *9*, 2289–2319. [CrossRef] [PubMed]
29. Mao, A.; Li, H.; Yu, L.; Hu, X. Electrochemical sensor based on multi-walled carbon nanotubes and chitosan-nickel complex for sensitive determination of metronidazole. *J. Electroanal. Chem.* **2017**, *799*, 257–262. [CrossRef]
30. Holanda, L.F.; Ribeiro, F.W.P.; Sousa, C.P.; Casciano, P.N.S.; De Lima-Neto, P.; Correia, A.N. Multi-walled carbon nanotubes-cobalt phthalocyanine modified electrode for electroanalytical determination of acetaminophen. *J. Electroanal. Chem.* **2016**, *772*, 9–16. [CrossRef]
31. Montes, R.H.O.; Lima, A.P.; Cunha, R.R.; Guedes, T.J.; Dos Santos, W.T.P.; Nosso, E.; Richter, E.M.; Munoz, R.A.A. Size effects of multi-walled carbon nanotubes on the electrochemical oxidation of propionic acid derivative drugs: Ibuprofen and naproxen. *J. Electroanal. Chem.* **2016**, *775*, 9–16. [CrossRef]
32. Pavinatto, A.; Mercante, L.A.; Leandro, C.S.; Mattoso, L.H.C.; Correa, D.S. Layer-by-Layer assembled films of chitosan and multi-walled carbon nanotubes for the electrochemical detection of 17α-ethinylestradiol. *J. Electroanal. Chem.* **2015**, *755*, 215–220. [CrossRef]
33. Chen, L.; Li, K.; Zhu, H.; Meng, L.; Chen, J.; Li, M.; Zhu, Z. A chiral electrochemical sensor for propranolol based on multi-walled carbon nanotubes/ionic liquids nanocomposite. *Talanta* **2013**, *105*, 250–254. [CrossRef] [PubMed]
34. Hundari, F.F.; Souza, J.C.; Zanoni, M.V.B. Adsorptive stripping voltammetry for simultaneous determination of hydrochlorothiazide and triamterene in hemodialysis samples using a multi-walled carbon nanotube-modified glassy carbon electrode. *Talanta* **2018**, *179*, 652–657. [CrossRef] [PubMed]
35. Zhai, H.; Wang, H.; Wanh, S.; Chen, Z.; Wang, S.; Zhou, Q.; Pan, Y. Electrochemical determination of mangiferin and icariin based on Au-AgNPs/MWNTs-SGSs modified glassy carbon electrode. *Sens. Actuators B Chem.* **2018**, *255*, 1771–1780. [CrossRef]

36. Yang, X.; Yu, X.; Heng, Y.; Wang, F. Facile fabrication of 3D graphene-multi walled carbon nanotubes network and its use as a platform for natamycin detection. *J. Electroanal. Chem.* **2018**, *816*, 54–61. [CrossRef]
37. Deng, K.; Liu, X.; Li, C.; Hou, Z.; Huang, H. An electrochemical omeprazole sensor based on shortened multi-walled carbon nanotubes-Fe_3O_4nanoparticles and poly(2,6-pyridinedicarboxylic acid). *Sens. Actuators B Chem.* **2017**, *253*, 1–9. [CrossRef]
38. Khaled, E.; Khalil, M.M.; El Aziz, G.M.A. Calixarene/carbon nanotubes based screen printed sensors for potentiometric determination of gentamicin sulphate in pharmaceutical preparations and spiked surface water samples. *Sens. Actuators B Chem.* **2017**, *244*, 876–884. [CrossRef]
39. Başkaya, G.; Yıldız, Y.; Savk, A.; Okyay, T.O.; Eriş, S.; Sert, H.; Şen, F. Rapid, sensitive, and reusable detection of glucose by highly monodisperse nickel nanoparticles decorated functionalized multi-walled carbon nanotubes. *Biosens. Bioelectron.* **2017**, *91*, 728–733. [CrossRef] [PubMed]
40. Wang, D.; Huang, B.; Liu, J.; Guo, X.; Abudukeyoumu, G.; Zhang, Y.; Ye, B.-C.; Li, Y. A novel electrochemical sensor based on Cu@Ni/MWCNTs nanocomposite for simultaneous determination of guanine and adenine. *Biosens. Bioelectron.* **2018**, *102*, 389–395. [CrossRef] [PubMed]
41. Li, J.; Lee, E.-C. Functionalized multi-wall carbon nanotubes as an efficient additive for electrochemical DNA sensor. *Sens. Actuators B Chem.* **2017**, *239*, 652–659. [CrossRef]
42. Ma, Y.; Shen, X.-L.; Zeng, Q.; Wang, H.-S.; Wang, L.-S. A multi-walled carbon nanotubes based molecularly imprinted polymers electrochemical sensor for the sensitive determination of HIV-p24. *Talanta* **2017**, *164*, 121–127. [CrossRef] [PubMed]
43. Anirudhan, T.S.; Alexander, S. A potentiometric sensor for the trace level determination of hemoglobin in real samples using multiwalled carbon nanotube based molecular imprinted polymer. *Eur. Polym. J.* **2017**, *97*, 84–93. [CrossRef]
44. Gutierrez, F.A.; Rubianes, M.D.; Rivas, G.A. Electrochemical sensor for amino acids and glucose based on glassy carbon electrodes modified with multi-walled carbon nanotubes and copper microparticles dispersed in polyethylenimine. *J. Electroanal. Chem.* **2016**, *765*, 16–21. [CrossRef]
45. Ji, J.; Zhou, Z.; Zhao, X.; Sun, J.; Sun, X. Electrochemical sensor based on molecularly imprinted film at Au nanoparticles-carbon nanotubes modified electrode for determination of cholesterol. *Biosens. Bioelectron.* **2015**, *66*, 590–595. [CrossRef] [PubMed]
46. Taurino, I.; Van Hoof, V.; De Micheli, G.; Carrara, S. Superior sensing performance of multi-walled carbon nanotube-based electrodes to detect unconjugated bilirubin. *Thin Solid Films* **2013**, *548*, 546–550. [CrossRef]
47. Sharma, V.V.; Gualandi, I.; Vlamidis, Y.; Tonelli, D. Electrochemical behavior of reduced graphene oxide and multi-walled carbon nanotubes composites for catechol and dopamine oxidation. *Electrochim. Acta* **2017**, *246*, 415–423. [CrossRef]
48. Li, J.; Sun, Q.; Mao, Y.; Bai, Z.; Ning, X.; Zheng, J. Sensitive and low-potential detection of NADH based on boronic acid functionalized multi-walled carbon nanotubes coupling with an electrocatalysis. *J. Electroanal. Chem.* **2017**, *794*, 1–7. [CrossRef]
49. Wayu, M.B.; DiPasquale, L.T.; Schwarzmann, M.A.; Gillespie, S.D.; Leopold, M.C. Electropolymerization of β-cyclodextrin onto multi-walled carbon nanotube composite films for enhanced selective detection of uric acid. *J. Electroanal. Chem.* **2016**, *783*, 192–200. [CrossRef]
50. Tarditto, L.V.; Arévalo, F.J.; Zon, M.A.; Ovando, H.G.; Vettorazzi, N.R.; Fernández, H. Electrochemical sensor for the determination of enterotoxigenic *Escherichia coli* in swine feces using glassy carbon electrodes modified with multi-walled carbon nanotubes. *Microchem. J.* **2016**, *127*, 220–225. [CrossRef]
51. Sipa, K.; Brycht, M.; Leniart, A.; Urbaniak, P.; Nosal-Wiercińska, A.; Pałecz, B.; Skrzypek, S. β-Cyclodextrins incorporated multi-walled carbon nanotubes modified electrode for the voltammetric determination of the pesticide dichlorophen. *Talanta* **2018**, *176*, 625–634. [CrossRef] [PubMed]
52. Özcan, A.; Gürbüz, M. Development of a modified electrode by using a nanocomposite containing acid-activated multi-walled carbon nanotube and fumed silica for the voltammetric determination of clopyralid. *Sens. Actuators B Chem.* **2018**, *255*, 262–267. [CrossRef]
53. Ghodsi, J.; Rafati, A.A. A voltammetric sensor for diazinon pesticide based on electrode modified with TiO_2 nanoparticles covered multi walled carbon nanotube nanocomposite. *J. Electroanal. Chem.* **2017**, *807*, 1–9. [CrossRef]

54. Wei, X.-P.; Luo, Y.-L.; Xu, F.; Chen, Y.-S.; Yang, L.H. In-situ non-covalent dressing of multi-walled carbon nanotubes@titanium dioxides with carboxymethyl chitosan nanocomposite electrochemical sensors for detection of pesticide residues. *Mater. Des.* **2016**, *111*, 445–452. [CrossRef]
55. Ertan, B.; Eren, T.; Ermiş, İ.; Saral, H.; Atar, N.; Yola, M.L. Sensitive analysis of simazine based on platinum nanoparticles on polyoxometalate/multi-walled carbon nanotubes. *J. Colloid. Interface Sci.* **2016**, *470*, 14–21. [CrossRef] [PubMed]
56. Xuan, X.; Park, J.Y. A miniaturized and flexible cadmium and lead ion detection sensorbased on micro-patterned reduced graphene oxide/carbonnanotube/bismuth composite electrodes. *Sens. Actuators B Chem.* **2018**, *255*, 1220–1227. [CrossRef]
57. Roushani, M.; Saedi, Z.; Hamdi, F.; Dizajdizi, B.Z. Preparation an electrochemical sensor for detection of manganese (II) ions using glassy carbon electrode modified with multi walled carbon nanotube-chitosan-ionic liquid nanocomposite decorated with ion imprinted polymer. *J. Electroanl. Chem.* **2017**, *804*, 1–6. [CrossRef]
58. Firmino, M.L.M.; Morais, S.; Correia, A.N.; De Lima-Neto, P.; Carvalho, F.A.O.; Castro, S.S.L.; Oliveira, T.M.B.F. Sensor based on β-NiO_x hybrid film/multi-walled carbon nanotubes composite electrode for groundwater salinization inspection. *Chem. Eng. J.* **2017**, *323*, 47–55. [CrossRef]
59. Sudha, V.; Kumar, S.M.S.; Thangamuthu, R. Simultaneous electrochemical sensing of sulphite and nitrite on acid-functionalized multi-walled carbon nanotubes modified electrodes. *J. Alloys Compd.* **2018**, *749*, 990–999. [CrossRef]
60. Li, Q.; Zhang, Q.; Ding, L.; Zhou, D.; Cui, H.; Wei, Z.; Zhai, J. Synthesis of silver/multi-walled carbon nanotubes composite and its application for electrocatalytic reduction of bromate. *Chem. Eng. J.* **2013**, *217*, 28–33. [CrossRef]
61. Qiu, X.; Lu, L.; Leng, J.; Yu, Y.; Wang, W.; Jiang, M.; Bai, L. An enhanced electrochemical platform based on graphene oxide and multi-walled carbon nanotubes nanocomposite for sensitive determination of sunset yellow and tartrazine. *Food Chem.* **2019**, *190*, 889–895. [CrossRef] [PubMed]
62. Tang, J.; Jin, B. Poly (crystal violet)-Multi-walled carbon nanotubes modified electrode for electroanalytical determination of luteolin. *J. Electroanal. Chem.* **2016**, *780*, 46–52. [CrossRef]
63. Sharma, A.K.; Mahajan, A.; Bedi, R.K.; Kumar, S.; Debnath, A.K.; Aswal, D.K. Non-covalently anchored multi-walled carbon nanotubes with hexa-decafluorinated zinc phthalocyanine as ppb level chemiresistive chlorine sensor. *Appl. Surf. Sci.* **2018**, *427*, 202–209. [CrossRef]
64. Jesionek, M.; Nowak, M.; Mistewicz, K.; Kępińska, M.; Stróż, D.; Bednarczyk, I.; Paszkiewicz, R. Sonochemical growth of nanomaterials in carbon nanotube. *Ultrasonics* **2018**, *83*, 179–187. [CrossRef] [PubMed]
65. Bora, A.; Mohan, K.; Pegu, D.; Gohain, C.B.; Dolui, S.K. A room temperature methanol vapor sensor based on highlyconducting carboxylated multi-walled carbon nanotube/polyanilinenanotube composite. *Sens. Actuators B Chem.* **2017**, *253*, 977–986. [CrossRef]
66. Arévalo, F.J.; Osuna-Sánchez, Y.; Sandoval-Cortés, J.; Tocco, A.D.; Granero, A.M.; Robledo, S.N.; Zon, M.A.; Vettorazzi, N.R.; Martínez, J.L.; Segura, E.P.; et al. Development of an electrochemical sensor for the determination of glycerol based on glassy carbon electrodes modified with a copper oxide nanoparticles/multiwalled carbon nanotubes/pectin composite. *Sens. Actuators B Chem.* **2017**, *244*, 949–957. [CrossRef]
67. Yu, H.; Feng, X.; Chen, X.-X.; Qiao, J.-L.; Gao, X.-L.; Xu, B.; Gao, L.-J. Electrochemical determination of bisphenol A on a glassy carbon electrode modified with gold nanoparticles loaded on reduced graphene oxide-multi walled carbon nanotubes composite. *Chin. J. Anal. Chem.* **2017**, *45*, 713–720. [CrossRef]
68. Hu, J.; Zhao, Z.; Zhang, J.; Li, G.; Li, P.; Zhang, W.; Lian, K. Synthesis of palladium nanoparticle modified reduced graphene oxide and multi-walled carbon nanotube hybrid structures for electrochemical applications. *Appl. Surf. Sci.* **2017**, *396*, 523–529. [CrossRef]
69. Wang, C.; Zhang, K.; Zhang, N.; Zhang, L.; Wang, H.; Xu, J.; Shi, H.; Zhuo, X.; Qin, M.; Wu, X. A simple strategy for fabricating a prussian blue/chitosan/carbon nanotube composite and its application for the sensitive determination of hydrogen peroxide. *Micro Nano Lett.* **2016**, *12*, 23–26. [CrossRef]